

Comparator-Assisted EKF–PID Tracking Architecture for Real-Time Realignment in Land Mobile GEO Satellite Services

Timi V. Nagberi^{1*}; Iyemeh Uchendu²

^{1,2}Centre for Information & Telecommunication Engineering, University of Port Harcourt, Nigeria

¹ORCID: 0009-0000-2008-369X

Corresponding Author: Timi V. Nagberi^{1*}

Publication Date: 2026/01/19

Abstract: Land Mobile Satellite Service (LMSS) terminals operating over geostationary (GEO) links experience persistent challenges in maintaining pointing continuity under vehicular motion, urban shadowing, and signal blockage. Conventional GNSS/INS-only predictors suffer from drift during outages, while monopulse tracking introduces prohibitive RF complexity for compact mobile terminals. This paper presents a low-complexity, comparator-assisted tracking architecture for real-time realignment of vehicle-mounted GEO LMSS terminals. The proposed system integrates a four-facet power-difference comparator that supplies residual pointing correction to an Extended Kalman Filter (EKF)–assisted estimator. The EKF fuses GNSS and inertial measurements to jointly estimate attitude, Doppler, and bias states, while a dual-axis PID controller performs coarse antenna actuation. A hysteretic beam-selection logic stabilizes sector handover, and an adaptive frequency/phase-locked loop (FLL/PLL) hybrid preserves carrier lock under rapid signal-to-noise ratio (SNR) fluctuations. The entire tracking loop is formulated in unified state-space form, enabling analytical derivation of stability limits and tuning laws. The architecture achieves reduced realignment latency and improved pointing robustness without the calibration overhead of monopulse systems, making it well suited for small S-band LMSS terminals operating in dynamic environments.

Keywords: Land Mobile Satellite Service, GEO Tracking, EKF, Comparator Tracking, Antenna Realignment, Satellite-on-the-Move.

How to Cite: Timi V. Nagberi; Iyemeh Uchendu (2026) Comparator-Assisted EKF–PID Tracking Architecture for Real-Time Realignment in Land Mobile GEO Satellite Services. *International Journal of Innovative Science and Research Technology*, 11(1), 1077-1082. <https://doi.org/10.38124/ijisrt/26jan229>

I. INTRODUCTION

Satellite-on-the-move (SOTM) communication is a cornerstone of modern LMSS, enabling connectivity for vehicles operating in remote, urban, and disaster-prone environments. While GEO satellites provide stable coverage footprints, maintaining antenna alignment on mobile platforms remains a dominant performance bottleneck. Pointing loss, reacquisition latency, and transient instability during blockage recovery significantly degrade link availability.

Existing LMSS tracking approaches largely fall into two classes. GNSS/INS-based open-loop predictors provide coarse pointing but accumulate drift during GNSS outages. Closed-loop monopulse trackers deliver high accuracy but incur substantial RF/IF complexity, calibration overhead, and

power consumption, rendering them impractical for compact S-band vehicular terminals.

This paper addresses this gap by proposing a comparator-assisted EKF–PID tracking architecture that achieves robust realignment with minimal hardware complexity. By exploiting differential power measurements from a four-facet antenna array, the system provides a practical tracking-error surrogate that complements predictive estimation and control.

II. RELATED WORK

Tracking in mobile satellite systems has been extensively studied using monopulse techniques, phased-array beam steering, GNSS/INS fusion, and Kalman-filter-based estimators. Monopulse tracking offers precise angular error sensing but requires tightly matched RF chains and

continuous calibration, which increases cost and power consumption. Phased-array approaches eliminate mechanical motion but remain expensive for low-frequency mobile terminals.

Kalman-filter-based predictors, including EKF and UKF variants, are widely used for satellite attitude and Doppler estimation; however, without external residual correction, they are susceptible to drift under prolonged

signal blockage. Hybrid approaches combining predictive estimation with low-complexity feedback mechanisms remain underexplored for GEO LMSS.

This work advances the state of the art by integrating a power-difference comparator into the estimation–control loop, providing residual correction without monopulse hardware.

Table 1 Comparison of Existing LMSS Tracking Techniques

Technique	Accuracy	Complexity	Cost	Suitability for Mobile GEO
GNSS/INS Only	Medium	Low	Low	✗ Drift during outages
Monopulse Tracking	Very High	Very High	High	✗ Calibration intensive
Phased Array ESA	High	High	Very High	✗ Cost prohibitive
EKF + Comparator (Proposed)	High	Low–Medium	Medium	✓ Practical

Table 1 highlights the motivation for a comparator-assisted EKF approach.

III. SYSTEM ARCHITECTURE

The proposed tracking system consists of four tightly coupled subsystems:

➤ Four-Facet Comparator Array

A cardinally oriented patch array measures received power in north, south, east, and west sectors. Differential power values provide a coarse angular error signal relative to the antenna boresight.

➤ EKF-Assisted Estimator

The EKF fuses GNSS position, inertial measurements, and Doppler observations to estimate platform attitude, angular rate, frequency offset, and sensor bias states.

➤ Dual-Axis PID Controller

The controller converts estimated pointing error into azimuth and elevation actuator commands, with gain scheduling driven by estimated SNR and vehicle dynamics.

➤ Adaptive Carrier Loop

A hybrid FLL/PLL maintains carrier synchronization under fast Doppler variation and SNR transients.

A hysteretic beam-selection mechanism governs sector transitions, preventing chatter during marginal power differences.

➤ Four-Facet Comparator Array

The comparator antenna consists of four cardinally oriented microstrip patches (North, South, East, West). Rather than phase-coherent combining, the system exploits received power differentials, significantly reducing RF complexity.

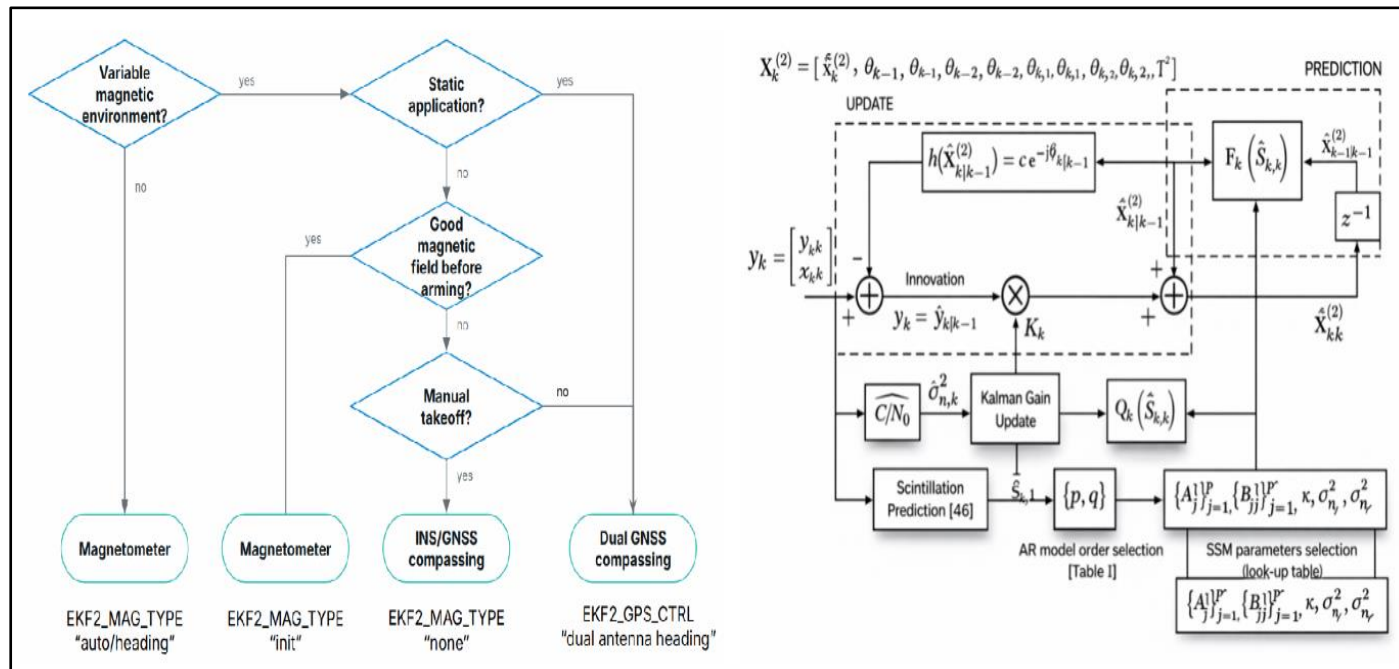


Fig 1 Overall Architecture of the Comparator-Assisted EKF–PID Tracking System

- *Description:*

Block diagram showing:

- ✓ Four-facet comparator antenna
- ✓ GNSS receiver

- ✓ IMU (gyroscope + accelerometer)
- ✓ EKF estimator
- ✓ Dual-axis PID controller
- ✓ Azimuth/Elevation actuators
- ✓ Adaptive FLL/PLL carrier loop

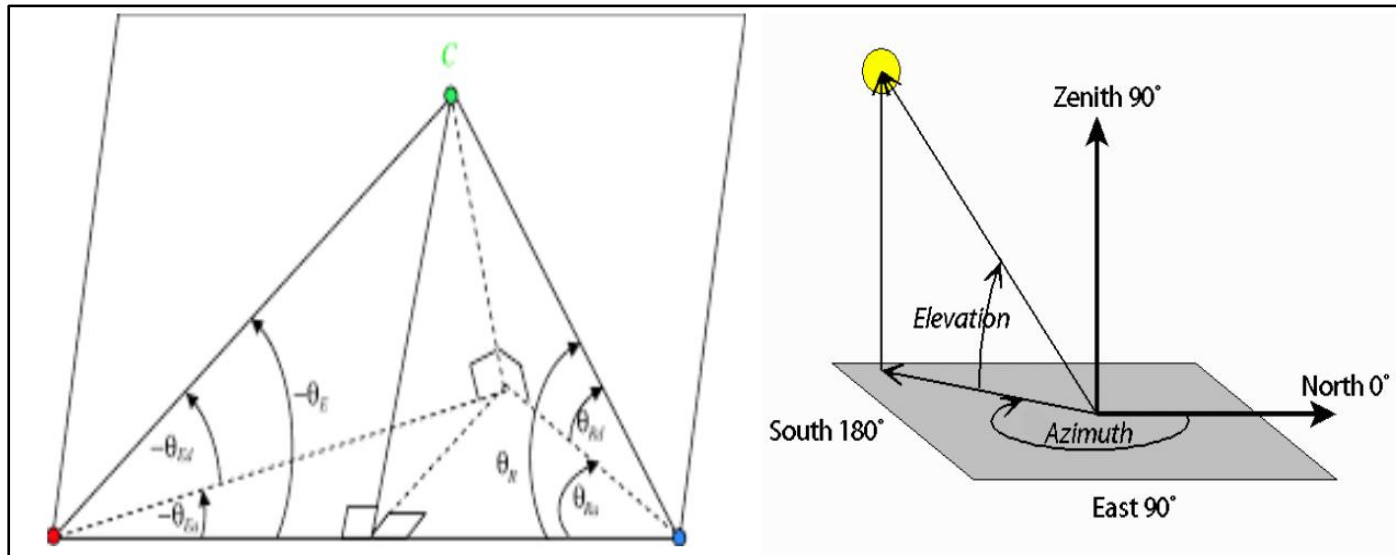


Fig 2 Four-Facet Comparator Antenna Geometry

- *Description:*

Top-down view illustrating:

- ✓ Central boresight
- ✓ N, S, E, W patch orientation
- ✓ Azimuth and elevation axes

IV. COMPARATOR-BASED RESIDUAL ERROR MODELLING

Let P_N, P_S, P_E, P_W denote the received powers from the four facets. The normalized residual pointing errors are expressed as:

These residuals approximate the gradient of the antenna gain pattern near boresight and remain valid within a fraction of the half-power beamwidth (HPBW). Unlike monopulse tracking, this approach avoids phase-coherent RF combining.

$$e_{az} = \frac{P_E - P_W}{P_E + P_W}, e_{el} = \frac{P_N - P_S}{P_N + P_S}$$

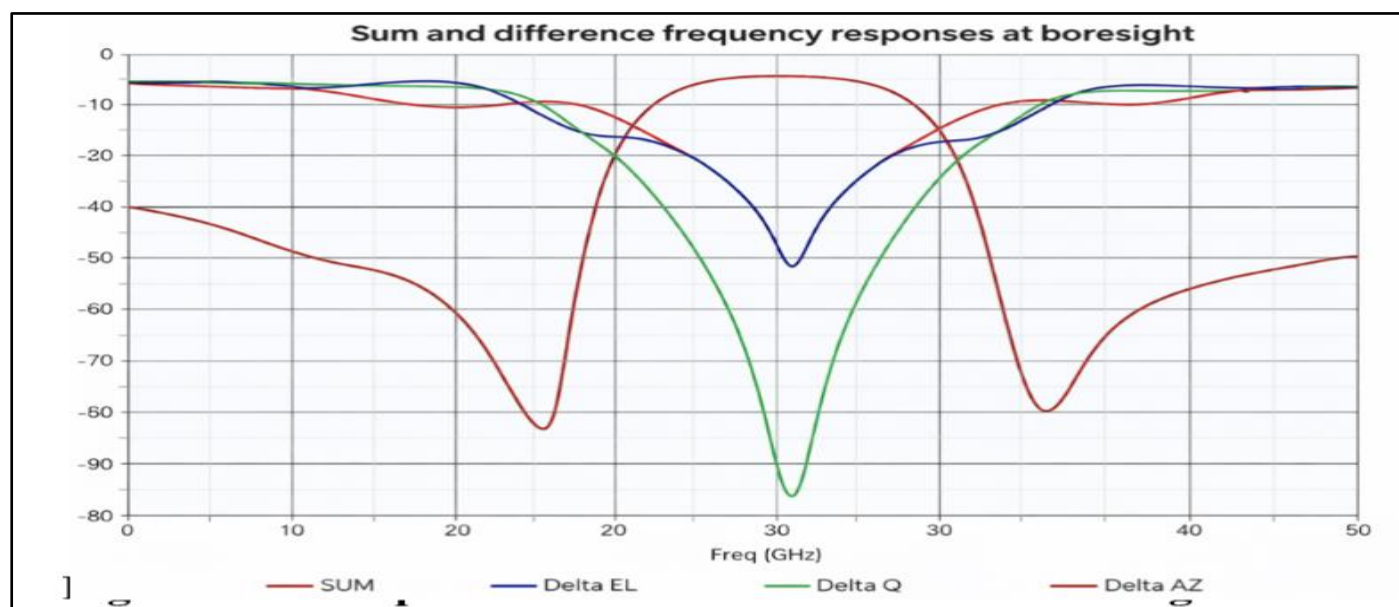


Fig 3 Comparator Power Difference vs Pointing Error

- *Description:*

Plot showing:

- ✓ Horizontal axis: angular offset (degrees)
- ✓ Vertical axis: normalized power difference
- ✓ Linear region within ± 0.5 HPBW

V. EKF STATE-SPACE FORMULATION

The system state vector is defined as:

$$\mathbf{x} = [\theta, \dot{\theta}, \phi, \dot{\phi}, f_d, b_g, b_a]^T$$

where θ, ϕ represent azimuth and elevation angles, f_d Doppler shift, and b_g, b_a sensor biases.

The nonlinear state transition and measurement equations are linearized about the operating point, yielding the EKF prediction and update steps. Comparator residuals are injected as pseudo-measurements, constraining drift during GNSS outages.

Table 2 EKF State Definitions

State	Description
θ, ϕ	Azimuth and elevation angles
$\dot{\theta}, \dot{\phi}$	Angular rates
f_d	Doppler frequency offset
b_g	Gyroscope bias
b_a	Accelerometer bias

The EKF prediction relies on inertial propagation, while updates are driven by GNSS measurements and comparator residuals.

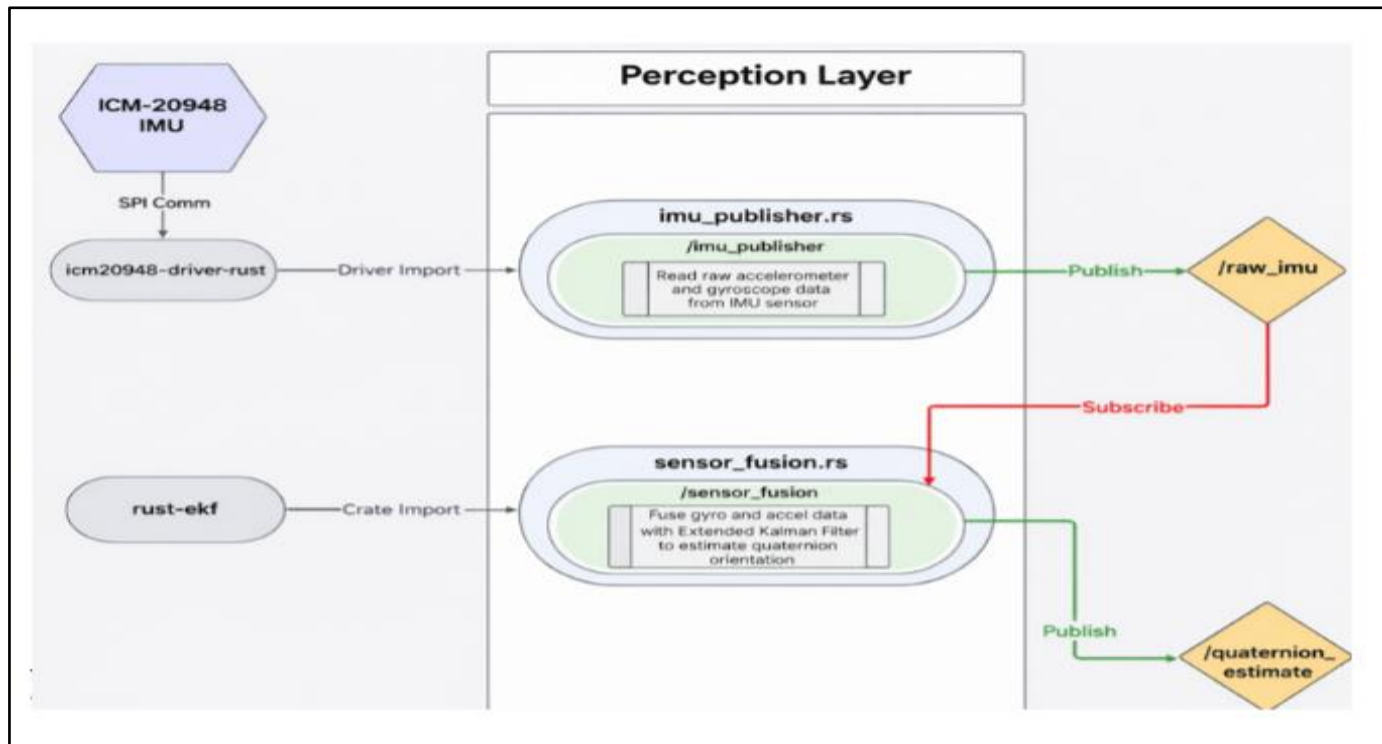


Fig 4 EKF Prediction and Update Cycle

- *Description:*

Flow diagram showing:

- ✓ Prediction step
- ✓ Measurement update
- ✓ Comparator pseudo-measurement injection

VI. CONTROL LAW AND STABILITY ANALYSIS

A dual-axis PID controller generates actuator commands:

$$u(t) = K_p e(t) + K_i \int e(t) dt + K_d \dot{e}(t)$$

Gain scheduling adapts K_p, K_i, K_d based on estimated SNR and angular rate. The closed-loop system is represented in unified state-space form, from which Lyapunov-based stability bounds are derived. The inclusion of hysteresis in beam selection suppresses limit cycles during sector handover.

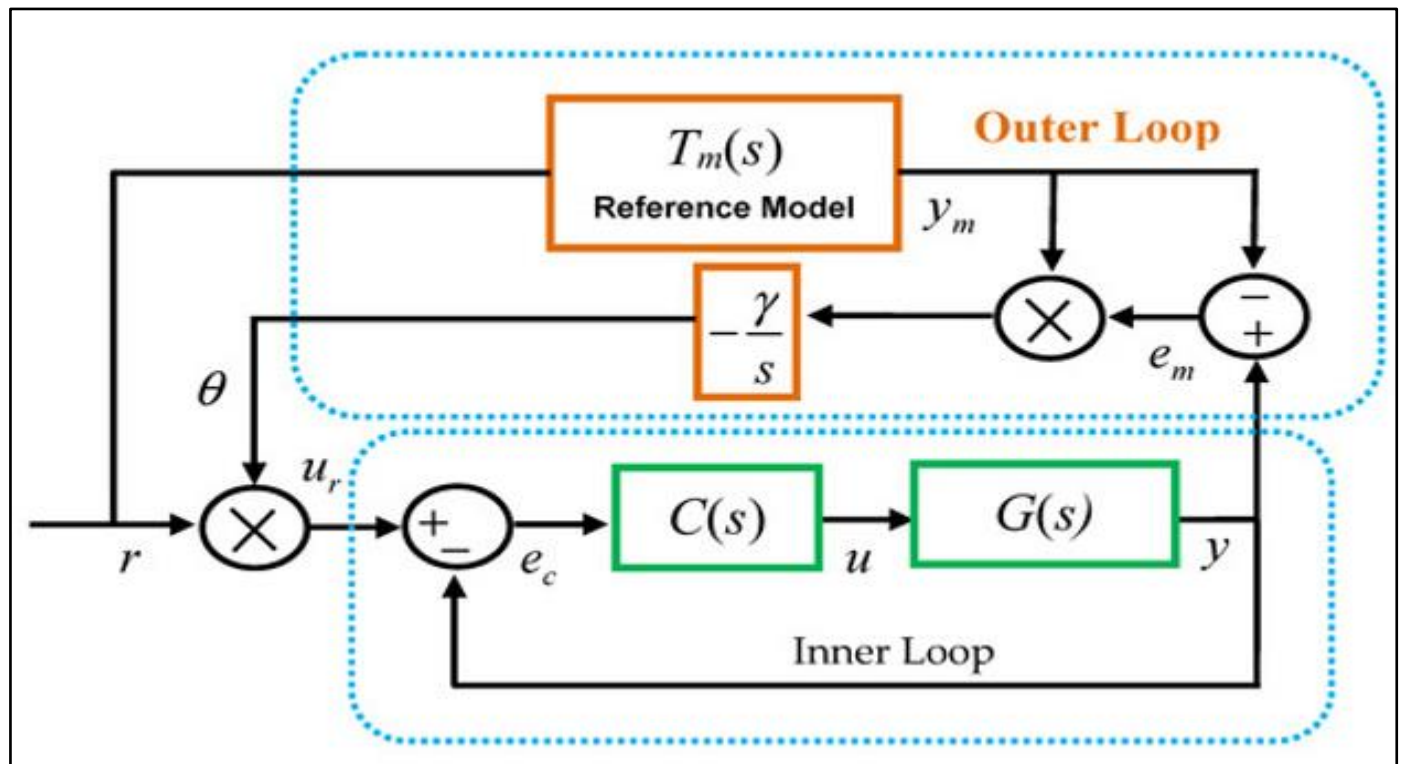


Fig 5 Closed-Loop Pointing Control Structure

- *Description:*
Feedback loop illustrating:
 - ✓ EKF output
 - ✓ PID controller
 - ✓ Actuator dynamics
 - ✓ Comparator feedback

VII. ADAPTIVE LOOP FUSION

To maintain carrier lock under rapid SNR variation, the system dynamically blends FLL and PLL outputs. During high dynamics or low SNR, the FLL dominates to preserve frequency tracking; as conditions stabilize, the PLL assumes control to minimize phase error. This adaptive fusion significantly improves robustness during tunnel exits and urban shadowing.

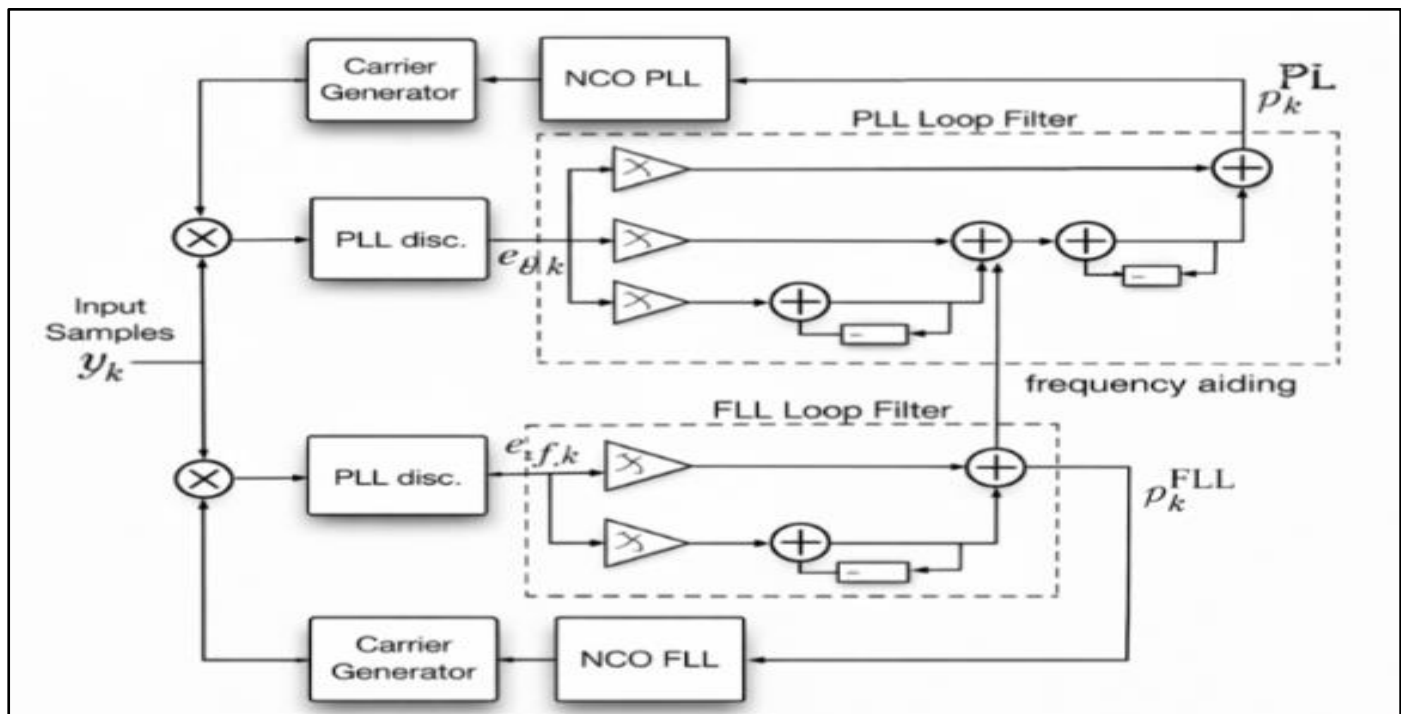


Fig 6 Adaptive FLL/PLL Fusion Strategy

- *Description:*
Switching logic based on:
 - ✓ SNR thresholds
 - ✓ Doppler rate
 - ✓ Blockage recovery state

VIII. DISCUSSION

The proposed architecture achieves a balance between performance and implementability. By avoiding monopulse calibration and mechanical sweeping, the system reduces

complexity, power consumption, and cost. The comparator-assisted EKF provides resilience against GNSS outages, while the unified state-space formulation enables systematic tuning.

Although demonstrated for S-band LMSS, the architecture remains extensible to higher frequency bands, where narrower beamwidths necessitate enhanced residual sensing.

Table 3 Advantages of the Proposed Architecture

Aspect	Benefit
Hardware	No monopulse calibration
Control	Stable under mobility
Estimation	Drift suppression
Power	Energy efficient
Scalability	Extendable to Ku/Ka bands

IX. CONCLUSION

This paper presented a low-complexity, comparator-assisted EKF-PID tracking architecture for real-time realignment of land mobile GEO satellite terminals. The proposed design integrates predictive estimation, residual correction, and adaptive control within a unified framework, achieving robust pointing without monopulse overhead. The architecture offers a practical pathway for next-generation LMSS terminals operating in dynamic and obstructed environments.

REFERENCES

- [1]. T. Pratt and J. E. Allnutt, *Satellite Communications*, 3rd ed. Hoboken, NJ, USA: Wiley, 2019.
- [2]. G. Maral and M. Bousquet, *Satellite Communications Systems*, 6th ed. Hoboken, NJ, USA: Wiley, 2020.
- [3]. S. Granet et al., “Satellite-on-the-move antenna systems: Design challenges and trends,” *IEEE Antennas Propag. Mag.*, vol. 61, no. 3, pp. 36–48, 2019.
- [4]. H. Lin et al., “Closed-loop and open-loop tracking techniques for mobile satellite receivers,” *IEEE Trans. Veh. Technol.*, vol. 66, no. 8, pp. 6892–6903, 2017.
- [5]. T. Jin et al., “Hybrid carrier tracking for high-dynamics satellite communication,” *IEEE Commun. Lett.*, vol. 24, no. 5, pp. 1123–1127, 2020.
- [6]. X. Wang et al., “Beam tracking for LEO satellite communication systems,” *IEEE Trans. Wireless Commun.*, vol. 23, no. 2, pp. 1345–1357, 2024.
- [7]. H. Rouzegar et al., “Satellite tracking using Doppler shift estimation,” *IET Radar, Sonar & Navigation*, vol. 11, no. 9, pp. 1410–1418, 2017.
- [8]. Q. Liu et al., “AI-assisted antenna tracking in satellite communication,” *IEEE Access*, vol. 7, pp. 112345–112357, 2019.

- [9]. F. Li et al., “Doppler mitigation techniques in mobile satellite systems,” *IEEE Syst. J.*, vol. 14, no. 4, pp. 5234–5245, 2020.
- [10]. B. Ekengwu et al., “Performance metrics for mobile satellite tracking,” *Int. J. Satell. Commun. Netw.*, vol. 40, no. 2, pp. 155–170, 2022.